Cancer Prognostics by Direct Detection of p53-Antibodies on Gold Surfaces by Impedance Measurements

Elisabet Prats-Alfonso,* Xavier Sisquella, Nadia Zine, Gemma Gabriel, Anton Guimerà, F. Javier del Campo, Rosa Villa, Adam H. Eisenberg, Milan Mrksich, Abdelhamid Errachid, Jordi Aguiló, and Fernando Albericio*

The identification and measurement of biomarkers is critical to a broad range of methods that diagnose and monitor many diseases. Serum auto-antibodies are rapidly becoming interesting targets because of their biological and medical relevance. This paper describes a highly sensitive, label-free approach for the detection of p53-antibodies, a prognostic indicator in ovarian cancer as well as a biomarker in the early stages of other cancers. This approach uses impedance measurements on gold microelectrodes to measure antibody concentrations at the picomolar level in undiluted serum samples. The biosensor shows high selectivity as a result of the optimization of the epitopes responsible for the detection of p53-antibodies and was validated by several techniques including microcontact printing, self-assembled-monolayer desorption ionization (SAMDI) mass spectrometry, and adhesion pull-off force by atomic force microscopy (AFM). This transduction method will lead to fast and accurate diagnostic tools for the early detection of cancer and other diseases.

1. Introduction

The identification and measurement of biomarkers is critical to a broad range of methods that diagnose and monitor many diseases.[1–3] Proteins are the most widely used and studied biomarkers, as shown in the literature[4–6] but serum auto-antibodies are rapidly becoming interesting targets because of their biological and medical relevance.[7,8] Usually, the detection of such antibodies is performed by an enzyme-linked immunosorbent assay (ELISA)[9,10] or another optical-based

Dr. E. Prats-Alfonso, Prof. F. Albericio
Institute for Research in Biomedicine
Barcelona Science Park
University of Barcelona
Baldiri Reixac 10, 08028-Barcelona, Spain
E-mail: epratsal@gmail.com; albericio@irbbarcelona.org

Dr. E. Prats-Alfonso, Prof. F. Albericio
CIBER-BBN, Barcelona Science Park
University of Barcelona
Baldiri Reixac 10, 08028, Barcelona, Spain

Dr. E. Prats-Alfonso, Prof. F. Albericio
Department of Organic Chemistry
University of Barcelona
Martí i Franqués 1-11, 08028-Barcelona, Spain

Dr. X. Sisquella
Nanotechnology Platform
Barcelona Science Park
University of Barcelona
Baldiri Reixac 10, 08028-Barcelona, Spain

Dr. N. Zine, Prof. A. Errachid
Université Lyon, Université Claude Bernard-Lyon 1
UMR 5180 institut des Sciences Analytiques
Bat CPE, 43, Bd du 11 novembre 1918, 69622,
Villeurbanne Cedex, France

Dr. G. Gabriel, A. Guimerà, Dr. F. J. del Campo,
Dr. R. Villa, Prof. J. Aguiló
Institut de Microelectrònica de Barcelona (IMB-CNM)
CSIC, Campus Universitat Autònoma de Barcelona
Barcelona 08193, Spain

Dr. A. H. Eisenberg, Prof. M. Mrksich
Howard Hughes Medical Institute and Northwestern University
Departments of Chemistry and Biomedical Engineering
2145 Sheridan Road, Evanston IL 60208

technology,[11,12] but these methods tend to suffer from low sensitivity and require a fluorescently labeled secondary antibody. Therefore, highly sensitive and direct detection methods[13] for antibodies would represent a significant advance in the early detection of cancer and other diseases.[1,3]

This article describes the direct detection of an unlabeled[14] primary antibody by impedance measurements in undiluted serum samples. We describe a new type of biosensor for the detection of p53 antibodies bound to peptides immobilized on functionalized gold microelectrodes. We are using antibodies as they are large, which is an ideal trait for electrical impedance detection as this is dependent on the analyte's size.[15] This technique relies on a charged surface to present either an attractive or repulsive force on ions near the microelectrode. Other factors, such as the temperature, pH, or size of the target, can modify the charge-transfer resistance, R_{ct},[14] so that the values of R_{ct} can be correlated to the concentration of the specific antibodies immobilized on the surface for a given set of environmental conditions. Antibodies also bind their target antigens with high specificity so that a highly selective sensor is obtained. Finally, antibodies are readily adapted to non-invasive and standard formats that are used in a traditional point-of-care environment. We are using the p53-protein, described as "the guardian of the genome", as it is crucial in the regulation of the cell cycle and acts as a tumor suppressor.[16] Its antibody (anti-p53) is also an attractive biomarker for characterizing several types of cancer, including ovarian cancer,[17,18] colorectal cancer,[19,20] and breast cancer.[21–25] Hence, this work serves as a diagnostic and prognostic tool for physicians to be used in combination with other conventional tumor marker tests[26] for the early detection of cancer.

2. Results

2.1. Epitopes Synthetic Design

We designed and synthesized several peptides based on the pentapeptide D-L-W-K-L (aspartic acid–leucine–tryptophan–lysine–leucine) that was identified as a reactive epitope of p53 in a phage display[27,28] (**Figure 1**a,b) (Supporting Information, S1). As described by Lane and co-workers this pentapeptide was the minimum expression to recognize the p53 antibody, although they use longer peptides in their arrays, they illustrate that this pentapeptide is the minimal requirement for recognition, which is the reason why our design is based on several approaches all containing this epitope.
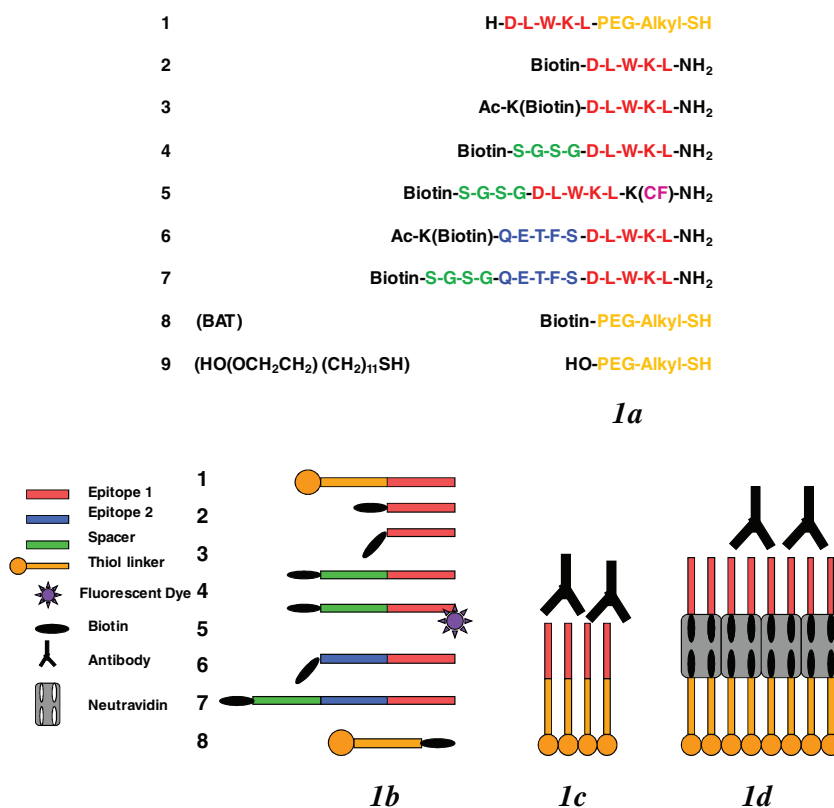

Figure 1. Peptide derivatives: a) Sequences (compounds show the reactive epitope in red, the longest reactive epitope in blue, and the linker in green; compound **1** includes an alkyl-PEG linker in orange). b) Schematic representations of peptides. c) Compound **1** attached to the gold surface through its own alkyl-PEG-thiol linker. d) Compounds **2**–**7** attached to the gold surface, which contains the BAT linker through a biotin/neutravidin complex.

Compound **1** incorporates an alkanethiol group, to form self-assembled monolayers (SAMs) on gold-coated substrates.[29–31] The ethylene glycol oligomer (polyethylene glycol, PEG) serves to limit the non-specific adsorption of proteins to the surface[32] (Figure 1c). The remaining compounds, **2**–**7**, have a biotin group incorporated into them so they can be bound to the gold surface through a neutravidin/biotin linkage. Compound **2** and **3** contain only the key pentapeptide with biotin at the N-terminal. The biotin on compound **3** is bound through the side-chain of an extra Lys residue in order to provide improved exposure of the peptide to the antibody. Compound **4** contains an extra spacer comprising the Gly-Ser repeat, which has previously been proposed in order to separate the epitope from the recognition sequence of detection.[27] Compound **5** is an analogue of **4**, but with a fluorescent tag at the C-terminal to visualize the surface after incubation with the peptide. Compounds **6** and **7** have an extra reactive epitope, with the aim to enhance the detection of the antibody.[27] To immobilize compounds **2**–**7**, a biotin alkyl thiol (BAT, **8**) was first incorporated onto the gold surface (Figure 1d). Compound **9** was used to block the untreated portions of the gold surface after peptide immobilization.

The advantage of compound **1** is that for the first time the peptide is already coupled to the alkyl thiol before attachment of the thiol on the surface. The obtention of the entire

compound (PEG-alkyl thiol + peptide) without the necessity of reactions over the surface makes the SAMs more repetitive, which makes the electrochemical impedance (EIS) measurements more reliable as these can be affected by the SAM formation.[33]

2.2. Specificity Inspection by Surface Immobilization

To verify the capability of the sensor system for qualitative detection, several assays with different techniques such as microcontact printing, self-assembled-monolayer desorption ionization (SAMDI) and atomic force microscopy (AFM) were performed.

For the first technique all immobilization reactions were compared relative to a "control" surface. This control consisted of first patterning the peptides on the gold surface using microcontact printing, after which the remaining surface was first blocked with HO-Peg-alkyl-SH (**9**) and then a fluorescently labeled secondary antibody was added. This "control" surface was used to monitor any interactions of the fluorescent reporter with the base sequences or with the surface,[29] and it was subtracted from all the resulting experiments to distinguish the specific immobilization of the fluorescently labeled antibody to our surface from other, non-specific interactions.

To test our biosensor, a monolayer was first patterned with **1**, treated with the primary anti-p53 antibody, and then with a second, fluorescently labeled antibody. We found that the secondary antibody strongly associated with the regions of the monolayer that were patterned with the peptide (**Figure 2**a). In a second experiment, we used microcontact printing to add the biotin alkanethiol (BAT) to the surface, and then this surface was treated with neutravidin and then the fluorescently labeled peptide **5**. Figure 2b shows that the immobilization of the peptide was indeed confined to the regions of the monolayer patterned with the biotin group. Finally, we prepared a monolayer of compound **4** patterned by way of the neutravidin/biotin, and we confirmed that this compound supported the binding of the secondary antibody. We note that the rest of the gold surface was blocked by **9** to prevent non-specific adsorption. In both cases (Figure 2a and 2c), the fluorescently labeled secondary antibody was detected.

The SAMDI method, which uses mass spectrometry to directly observe the alkanethiols of the monolayer and proteins that are associated with the monolayer,[34] was used as additional confirmation of antibody binding. We performed assays on a glass slide having an array of gold spots (**Figure 3**a), that were modified with a monolayer presenting either compound **1** or BAT (**8**) mixed with **9**, in a ratio of 1:9. The surfaces were treated with antibodies against **1** or with neutravidin,
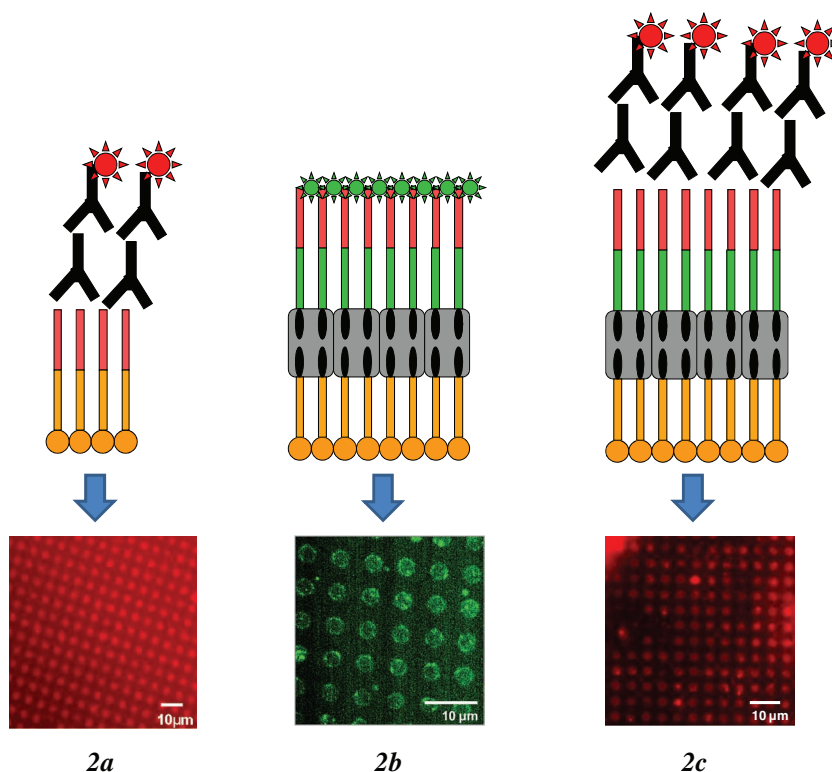

Figure 2. Microcontact printing: a) **1** incubated first with the primary antibody and then with the fluorescently labeled secondary antibody. b) Immobilization of one biotin compound **5** to check the first part of the process. c) BAT incubated with neutravidin and **4**, and subsequent incubation with fluorescently labeled secondary antibody.

compounds (**2**–**7**), and then analyzed by SAMDI. In each case, the spectra were consistent with the design of the assay. Notably, the bound antibodies, having molecular weights of approximately 150 kDa were clearly identified in the SAMDI spectra (Supporting Information, S2). In experiments 1D and XF, the antibody against human serum albumin (HSA) was used instead of p53 because HSA is the most abundant protein in blood,[35] and its antibody could be one of the possible interferences in the detection system. In these experiments no signal was observed (Figure 3b-e), showing that the assay was specific for anti-p53.

In addition to fluorescence assays and SAMDI-MS, we used AFM to probe the strength and specificity of the interactions of surface bound peptides **1**–**4** and **7** with the labeled antibodies (Supporting Information, S3). To do this, anti-p53 was first immobilized on the tip of the AFM cantilever through a bifunctional PEG linker. The tip was then brought into contact with the peptide-functionalized surfaces to yield the antibody complex. The tip was then pulled away from the surface, and the resulting force was measured. In doing so, we were able to evaluate the strength, and thus specificity, of the antibody binding.

The images show (**Figure 4**) that compound **1** (without the neutravidin-biotin system) and the peptides with the spacer (green) (**4** and **7**) gave the best image of the pattern in the adhesion pull-off force map, where we can see clearly patterned peptides. In contrast, compounds **2** and **3** without a spacer or with only a single lysine residue gave the poorest maps (absence of defined patterned spots).
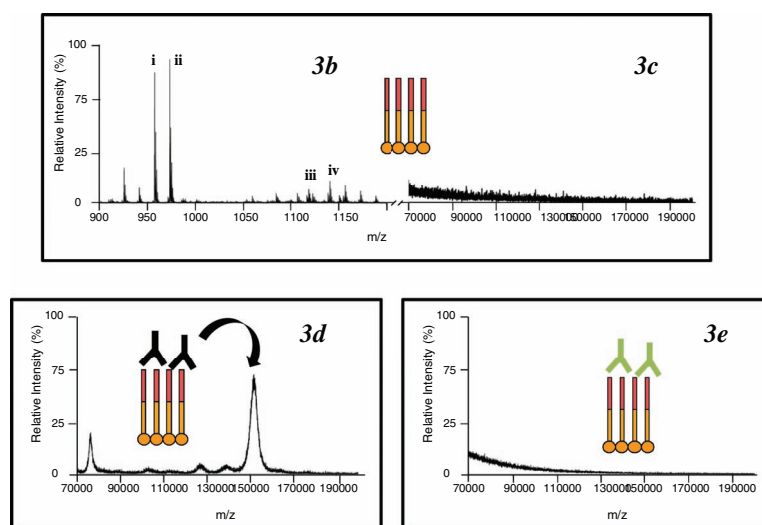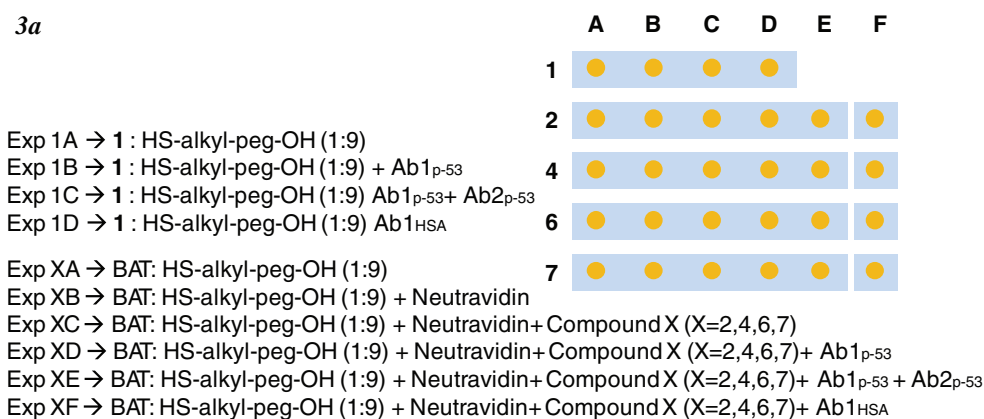
3a

Exp 1A → **1** : HS-alkyl-peg-OH (1:9)
Exp 1B → **1** : HS-alkyl-peg-OH (1:9) + Ab1$_{p-53}$
Exp 1C → **1** : HS-alkyl-peg-OH (1:9) Ab1$_{p-53}$+ Ab2$_{p-53}$
Exp 1D → **1** : HS-alkyl-peg-OH (1:9) Ab1$_{HSA}$

Exp XA → BAT: HS-alkyl-peg-OH (1:9)
Exp XB → BAT: HS-alkyl-peg-OH (1:9) + Neutravidin
Exp XC → BAT: HS-alkyl-peg-OH (1:9) + Neutravidin+ Compound X (X=2,4,6,7)
Exp XD → BAT: HS-alkyl-peg-OH (1:9) + Neutravidin+ Compound X (X=2,4,6,7)+ Ab1$_{p-53}$
Exp XE → BAT: HS-alkyl-peg-OH (1:9) + Neutravidin+ Compound X (X=2,4,6,7)+ Ab1$_{p-53}$ + Ab2$_{p-53}$
Exp XF → BAT: HS-alkyl-peg-OH (1:9) + Neutravidin+ Compound X (X=2,4,6,7)+ Ab1$_{HSA}$

Figure 3. SAMDI mass spectrometry: a) Each glass slide is an experiment with one peptide. Experiment 1 was performed with compound **1** on the first slide, whereas the remaining experiments were carried out on the subsequent slides with the other compounds, (Experiment 2, compound **2**, and so on). Each spot represents one incubation, step by step, from left to right. Then each spot was analyzed by SAMDI and the mass spectra of each spot were acquired. The "F" experiments were carried out on different glass slides to avoid cross contamination with the p53 antibodies. b) SAMDI spectra: i) [$M_{HspegOH}$ x2+Na] = 958.0 Da, ii) [$M_{HspegOH}$ x2+K] = 973.7 Da, iii) [$M_{Hspegpeptide}$+Na] = 1118.9 Da, iv) [$M_{Hspegpeptide}$+K] = 1141.1 Da. c) SAMDI spectra showing higher masses with no molecules adsorbed in the first step. d) Mass of the primary antibody, (anti-p53) = 151 800 Da (M_w approx. 150kDa), e) No detection of anti-HSA.

We performed a more detailed study, analyzing all the data from each experiment. Each map has 4096 pixels, and each pixel represents a unique force curve. The force extension curve of the bifunctional PEG had a specific shape,[36] which allowed discrimination between non-specific adhesion and single molecule-specific adhesion between the antibody and the peptide. After checking all the curves, we calculated the probability of a specific interaction on the basis of the number of positive events in the white spots (Supporting Information, S4). We measured the adhesion pull-off force for two monolayers presenting compound **1** and obtained values of $1.7 \times 10^{-10} \pm 1.3 \times 10^{-11}$ N and $1.3 \times 10^{-10} \pm 2.9 \times 10^{-11}$ Da (significantly equals by t-student test).

To verify the specificity, three negative controls were performed for the whole experiment. The first test revealed almost no interaction between the antibody and **9**, in comparison with the peptides patterned, as the force map image shows. The second control was performed by attaching an unspecific antibody, the anti-HSA, to the tip of the cantilever to test its

specificity for the peptides in comparison to the specific antibody. A final control was a competition experiment. In this experiment, a peptide with only the target sequence (DLWKL) was dissolved in phosphate buffered saline (PBS) and added to the surface with immobilized peptide. In principle, if the recognition is specific, the soluble peptide should compete with the immobilized peptide and partly bind to the antibody, blocking the interaction between the peptide attached to the surface and the antibody situated at the tip allowing to calculate the probability of specific binding (**Figure 5**).

2.3. Stability Assays

As the detection was based on the incubation of the serum containing the antibody with the peptides immobilized on the surface of the biosensor, the stability of compounds **1** and **4** were studied in human serum for a period of 180 min.[37] Comparative results (Supporting
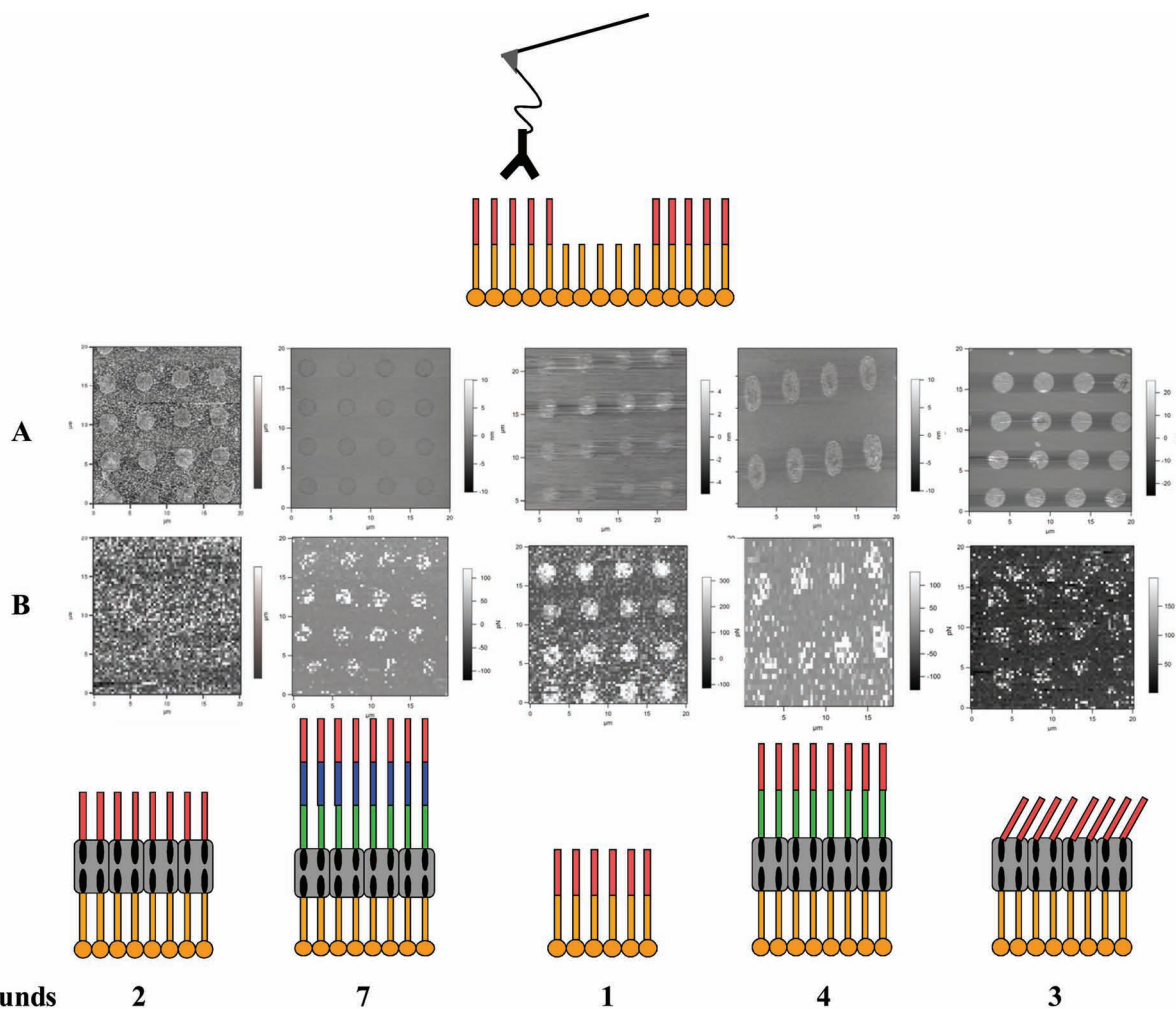
Figure 4. Adhesion pull-off force: A) Microcontact printing pattern by AFM (spots of 2.5 μm), B) force map of the adhesion pull-off force assay.

Information, S5) showed that compound **4** was more resistant to degradation, with a half-life of 38.5 h, whereas compound **1** had a half-life of 17.5 min. Although both peptides have considerably different stabilities in solution, their stabilities increase once attached to the surface of the biosensor which makes both peptides suitable for detection over the 2 h experiment.[21]

2.4. Impedance Measurements

This technique measures the presence of the biomarker by determinating the concentration of antibodies that specifically binds to the gold-coated surface after peptide immobilization. The electrochemical magnitude is determined by the electron transfer resistance caused by the formation
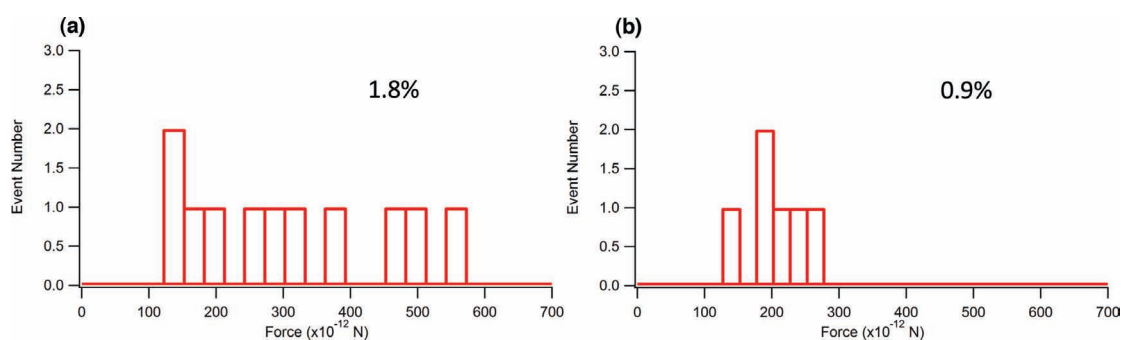

Figure 5. Corresponding histograms for surface with compound **1** (a) and negative control with the soluble peptide (b). The event number clearly decreases by half. The probability of specific bounding is 1.8% for (a) whereas for (b) it is 0.9%.

of antibody–peptide complexes on the microelectrode surface (Supporting Information, S6).

It is worthy to mention that many parameters, such as the ion capture or the antibody conformation, can modify the EIS values, which has been suggested by Bogomolova et al.[38] although the EIS technique is very powerful, some caution is required to verify that the results are not false positives.

The initial electrode contamination is crucial, so, as described in the experimental section, additional cyclic voltammetry was performed in order to check the gold surface. Repetitive measurements were carried out with the aim of corroborating the EIS results, so triplicates of each concentration step were made, using the average as the final value (solid line in the pictures, standard deviation in percentage can be found in the Supporting Information, S9-Table 1)

Some of the microelectrodes were incubated in a solution with a mixture of compound **1** and **9**, and others with BAT and HO-Peg-alkyl-SH (**9**) in the same proportion as used in the SAMDI assays to mimic the optimized conditions. The BAT incubations, as in the previous experiments, included the subsequent incubation with neutravidin and compound **4**.

In a first stage of the experiment, the assay was performed by adding the antibodies to a solution of PBS over a range of concentrations. Once the surfaces were coated, the antibody was incubated on the electrode and then measured by EIS.

The results show the capacity of the biosensor to specifically detect anti-p53 at a 6.67×10^{-17} M range (10 fg mL^{-1}) for both peptides (**Figure 6** and Supporting Information, S7) The large difference between the lowest concentration (10^{-17} M), red line in Figure 6, and the SAM used as reference, green line in Figure 6, indicates that it would be possible to further decrease the concentration.

Furthermore, we performed a study with the anti-HSA to establish whether non-specific antibodies show a distinct behavior (Supporting Information, S8). Whereas the binding of anti-p53 even at 10^{-17} M was much higher than that of the "SAM control", the binding of anti-HSA at 10^{-8} M was much lower than that of the control SAM. These results corroborate those found in the SAMDI assays, namely that the binding was extremely specific.

Given that the purpose of the biosensor is to be used with blood from patients, we conducted a final experiment to add the antibodies to undiluted human serum at a concentration of 6.67×10^{-12} M (1 ng mL^{-1}). This concentration was chosen because the limit for a healthy concentration in ovarian cancer has been established as 0.16 µg mL^{-1}.
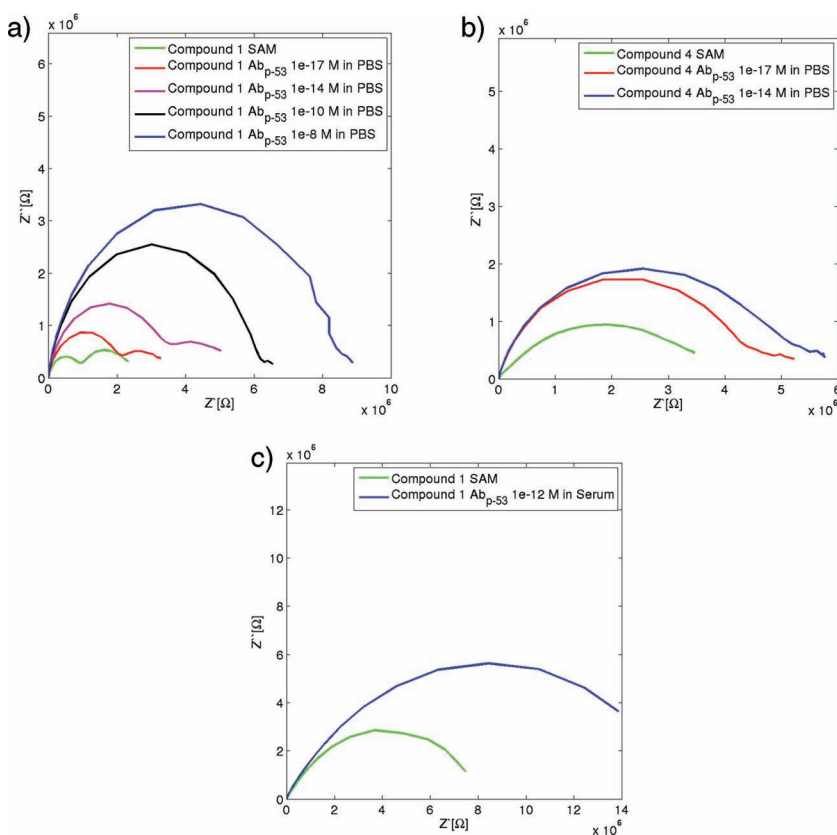

Figure 6. Nyquist plots for a) **1** and b) **4** at a range of different anti-p53 concentrations to verify that the system is able to quantify the concentration of anti-p53 in PBS buffer. a) **1**: Green: SAM control; red, pink, black, and blue: Ab$_{p-53}$ [10^{-17}], [10^{-14}], [10^{-10}], [10^{-8}] M in PBS, respectively. b) **4**: Green: SAM control, red and blue: Ab$_{p-53}$ [10^{-17}], [10^{-14}] M in PBS, respectively. c) Nyquist plot for the quantification of anti-p53 at a 10^{-12} M concentration in a serum fluid showing an approximation of the biosensor to be used in real human samples. The green line corresponds to the SAM control and the blue line corresponds to Ab$_{p-53}$ [10^{-12}] M in serum. (Solid line represents the average of triplicates, standard deviation in Supporting Information, S9-Table 1).

The system showed to work well to measure the antibody in serum (Figure 6c). Table 1 in the Supporting Information (S9) shows the R_{ct} values for different concentrations measured.

3. Discussion

The knowledge of anti-p53 levels are a crucial aid to monitoring the stages of the cancer disease, in several cancers. The principal aim of our work was to validate the interaction of the detection system and use this assessment to develop a biosensor.

Our results have shown the high specificity of the selected peptides towards the antibody by several techniques. The microcontact printing allowed us to visually check the specificity of the peptides, showing only the fluorescence of the labeled antibodies in the patterned surfaces, which implies that the primary antibody was specifically attached only to the regions where the epitope was deposited. In addition, the SAMDI technique provided us with clear evidence of the

minimal non-specific adsorption on the sensor and, consequently, the high specificity of the functionalized surface for the antibody.

Furthermore, the AFM force assays have allowed us to perform control experiments to confirm the standard of specificity and recognition of each peptide, using non-specific antibodies and competition assays that verify the robust sensor system. This approach allowed us to better understand the specificity of the system and to evaluate the recognition between the different peptides towards the antibody on a single-molecule level. Peptides with shorter linkers or without linkers gave poor recognition (absence of defined patterned spots). This observation can be justified, as is the case for the ELISA technique, by the fact that the peptide needs to be at a certain distance from the neutravidin to attain more efficient antibody–peptide recognition. The poor recognition of peptides with shorter or no linkers could be clearly seen in the adhesion force image, by analyzing the positive events. A positive event is defined as a specific interaction of the antibody towards the peptide, shown by the force curve shape as explained before (Supporting Information, S3). Also, the corresponding histograms were fitted with Gaussian curves to obtain the force data for each peptide. In contrast, for the experiments performed with HSA antibody an arithmetic average was used to calculate the force data because the number of positive events was very low, which again demonstrates the difference in specificity (Supporting Information, S4). The assays performed with anti-HSA (second control) gave values in force that differed significantly from those for the anti-p53 for compound **4**. This means that the specificity of the peptides towards both antibodies is different, unlike for compound **1**. When the competition control experiment was performed for compound **1** with anti-p53, the assay showed a force of $1.9 \times 10^{-10} \pm 1.7 \times 10^{-11}$ N, which is similar to the previous data. However, the probability of specific binding decreased by half in the competition experiment indicating that the presence of peptide in solution could interfere and partially block the antibody–(immobilized) peptide interaction (Figure 5).

The force calculated for **4**, **3**, and **7** was $2.0 \times 10^{-10} \pm 2.0 \times 10^{-11}$ N, $1.7 \times 10^{-10} \pm 0.9 \times 10^{-11}$ N, and $1.6 \times 10^{-10} \pm 1.2 \times 10^{-11}$ N, respectively. The values for **4** and **3** are in agreement with that measured for monolayers of compound **1**. The value for **7** differs significantly from the other peptides. This variance is attributed to the extended length of **7**, which likely confers different specificity properties toward the antibody.

We have demonstrated with this AFM assay that the designed peptides exhibit a specific recognition at the single-molecule level. All these results showed that in general, the differences, in terms of force, did not differ substantially. In this regard, compounds **1** and **4** were chosen because both behaved similarly, in terms of recognition and specificity, compared to the other peptides. Furthermore, they represent the two synthetic groups presented (**1** directly attached onto the gold surface and **4** biotinylated peptide attached through biotin/neutravidin system) and were relatively trivial to synthesize compared to the other peptides.

The stability assays in serum contributed to the whole validation for the future application of the biosensor. Having

confirmed the high specificity of the system by the absence of false positives, and the stability in the presence of the serum, we examined the interaction between the compounds (**1** and **4**) and the antibody by EIS.[39] The main reason for the improvement of the signal is the use of small epitopes, instead of the whole protein;[40] this created a difference in size between the probe and the target, thus allowing the impedance technique to achieve extremely high sensitivity in PBS. The selected concentration for serum detection was chosen for being near the cut-off values in ovarian cancer. However, as can be observed in the impedance curves, the wide range between the "SAM control" and the lower concentration in PBS (10^{-17} M), suggests that in serum it would also be possible to reduce the concentration of antibody below 10^{-12} M, because in the serum the difference between the SAM control and the measure is equally large. Experiments (Supporting Information, S8) demonstrated that 2 h is the most suitable length of incubation with the antibody, which is consistent with a previous report.[21] However, we firmly believe that a change in the percentage of peptide coating on the surface would allow a decrease in incubation time.

4. Conclusion

Our novel type of detection avoids the need of a sandwich assay and a fluorescently labeled antibody, thus giving the concentration of the antibody as a direct impedance signal. Compound **1** was relatively easy to synthesize and also to deposit on the surface. Moreover, as the whole protein was avoided and the number of steps reduced, the entire synthetic process, in cost and time, was significantly reduced. Finally, SAMs are very stable and can be preserved for about a month[41] thus providing a sensor that can be stored and ready for detection during a long period of time.

Here we developed and validated an impedance biosensor with a high selectivity and sensitivity for the label-free detection of anti-p53 in human serum. The design of this label-free, inexpensive and sensitive biosensor opens the way to the use of a wide range of antibody biomarkers to prepare biosensors that have the capacity to detect other immune illnesses. We are currently working on miniaturizing the device and instrumentation in order to make this biosensor available to physicians in hospitals for early cancer detection and other diseases.

5. Experimental Section

For chemicals, reagents and general synthesis instrumentation see Supporting Information.

Peptides Synthesis. General Procedures: The solid-phase synthesis was performed in polypropylene syringes (5–20 mL), each fitted with a polyethylene porous disk. For peptide **1** we used CTC (chlorotrityl chloride resin) (400 mg) with a functionality of 1.2 mmol g^{-1}. For the biotinylated compounds, the resin MBHA-Rink amide (amino-(4-methylphenyl)methyl polystyrene) was used with a functionality of 0.45 mmol g^{-1}. Solvents and soluble reagents were removed by suction. After the incorporation of the building block in the CTC resin, a capping step was performed

(200 μL MeOH−29 μL *N,N″*diisopropylethylamine (DIPEA)−100 mg resin). Fluorenylmethyloxycarbonyl (Fmoc) was removed with piperidine−dimethylformamide (DMF) (1:4, v/v) containing 1-hydroxybenzotriazole (HOBt) (1.3 M) (1 × 1 min, 2 × 10 min) in order to prevent aspartimide formation.[42] Resins were washed before use and between deprotection, coupling, and subsequent deprotection steps with DMF (3 × 30 s) and dichloromethane (DCM) (3 × 30 s) using 10 mL of solvent g^{-1} of resin each time.

All compounds were synthesized by standard synthesis using a DIPCDI (*N,N'*-diisopropylcarbodiimide)/HOBt protocol (aa, DIPCDI, and HOBt 3 eq. each in DMF), the biotin was coupled using 5 eq. For biotin incorporation in the lateral chain, an orthogonal protecting group of the amine of the lysine Alloc (allyloxycarbonyl) was removed with palladium *tetrakis*-triphenylphosphine in the presence of phenylsilane (10 eq.) and in DCM (3 × 15 min). BAT synthesis and the two first couplings of **1** were carried out as described previously.[32] For **1**, **3**, and **6** a final acetylation with 10% Ac$_2$O in DMF was performed before the cleavage.

The incorporation of the carboxyfluorescein (5 eq. as a fine powder)[43,44] was achieved through two couplings of 1.5 h and one of 16 h, respectively, with PyAOP ((7-azabenzotriazolo-1-yloxi)-tris(pirrolidino)phosphoniumhexafluorophosphate) (5 eq.), HOAt (5 eq.), DIPEA (10 eq.) in DMF (9:1) containing 1% of triton to disaggregate the compound, with 10 min of pre-activation.

Cleavage was performed using trifluoroacetic acid (TFA)−H$_2$O−triethylsilane (TES) (95:2.5:2.5, v/v) (1 h) followed by washings with the cocktail cleavage (3 × 1 min). The cleavage for **1** was performed with the cocktail R, TFA−thioanisole−ethandithiol (EDT)−anisole (90:5:3:2) and some drops of TES. The peptides were precipitated with diethyl ether, lyophilized, and purified when needed.

Characterization: (Supporting Information, S1.2): Compound **1**: Purity of 99% (after purification) t_R = 1.825 min, gradient: 20:80 to 60:40 (acetonitrile (ACN)/H$_2$O) in 8 min MALDI-TOF *m/z* calcd. for C$_{56}$H$_{95}$N$_9$O$_{12}$S, 1117.68, found 1118.5699 [M + H]$^+$; Compound **2**: Purity of 98% (t_R = 2.242 min, gradient: 30:70 to 70:30 (ACN/H$_2$O) in 8 min MALDI-TOF *m/z* calcd. for C$_{43}$H$_{66}$N$_{10}$O$_9$S, 898.47, found 899.3963 [M + H]$^+$; Compound **3**: Purity of 98% (after purification) t_R = 4.210 min, gradient: 20:80 to 60:40 (ACN/H$_2$O) in 8 min MALDI-TOF *m/z* calcd. for C$_{51}$H$_{80}$N$_{12}$O$_{11}$S, 1068.58, found 1069.5212 [M + H]$^+$; Compound **4**: Purity of 92% t_R = 3.673 min, gradient: 20:80 to 60:40 (ACN/H$_2$O) in 8 min MALDI-TOF *m/z* calcd. for C$_{53}$H$_{82}$N$_{14}$O$_{15}$S, 1186.58, found 1187.5496 [M+H]$^+$; Compound **5**: Purity of 68% (t_R = 4.583 min, gradient: 5:95 to 100:0 (ACN/H$_2$O) in 8 min MALDI-TOF *m/z* calcd. for C$_{80}$H$_{104}$N$_{16}$O$_{22}$S, 1672.72, found 1673.6179 [M + H]$^+$; Compound **6**: Purity of 92% (after purification) t_R = 4.820 min, gradient: 20:80 to 60:40 (ACN/H$_2$O) in 8 min HPLC-MS *m+z/z* calcd. for C$_{76}$H$_{114}$N$_{18}$O$_{21}$S, *z* = 1 1646.81, *z* = 2 found 823; Compound **7**: Purity of 92% (after purification) t_R = 2.735 min, gradient: 30:70 to 40:60 (ACN/H$_2$O) in 8 min MALDI-TOF *m/z* calcd. for C$_{79}$H$_{118}$N$_{20}$O$_{25}$S, 1778.83, found 1779.8872 [M + H]$^+$; Control peptide: Purity of 99% t_R = 3.525 min, gradient: 20:80 to 80:20 (ACN/H$_2$O) in 11 min HPLC-MS *m+z/z* calcd. for C$_{35}$H$_{54}$N$_8$O$_8$, 714.41, found 715.

Microcontact Printing: 1.1 mm float glass + 2 nm Ti + 40 nm Au gold surfaces were purchased from NTB Buchs, Switzerland. BAT (1 mM) and **1** (1mM) in EtOH was used to ink a 2.5 μm polydimethylsiloxane (PDMS)-positive stamp. Before thiol inking, the PDMS stamp was oxidized with O$_2$ plasma to ensure good coverage of

the stamp surface with the thiol. After keeping the stamp in contact with the gold surface, the samples were immersed in HO-PEG-alkyl-SH (2 mM diluted EtOH solution for 24 h). **9** prevented the non-specific adsorption of proteins on the non-functionalized gold areas (bovine serum albumin (BSA) gold blocking would also be effective). Samples with neutravidin (10^{-7} M) were incubated for 1 h at room temperature for the surfaces covered by BAT and subsequently incubated with biotin peptide derivatives (1 μM) during 2 h at 4 °C. The incubation with the antibodies, labeled or not, was performed at a concentration of 10^{-8} M for 2 h at 4°C.

The images were obtained using an Eclipse E1000 upright microscope (Nikon, Netherlands), working with a G-2A filter to observe the red fluorescence from the secondary antibody labeled with Texas-red. For the image of **5**, UV-cleaned glass slides (150 μm thickness) were coated with a Ti/Au layer (2 nm/10 nm) by thermal evaporation.

The peptide labeled with carboxyfluorescein was excited using the 488 nm line of an argon/krypton-ion laser (CW, Spectra-Physics). The circularly polarized excitation light was focused onto the sample using an oil immersion objective (100×, 1.3 NA). The emitted fluorescence was collected and spectrally separated from the excitation light using a Brightline FF01 536/40 nm, 25 end, 15 μW (488 excitation) 30 μm × 30 μm filter. The signals were sent to photon-counting avalanche photodiodes (APDs).

SAMDI: *Preparation of Gold Substrates*:[45,46] Glass coverslips were sonicated for 30 min first in deionized ultrafiltered (DIUF) water and then in EtOH. They were then dried under a stream of nitrogen. Titanium (4 nm) and gold (22 nm) were evaporated onto the glass coverslips using an electron beam evaporator (Thermionics) at a rate of 0.2 nm s^{-1} and 0.4–0.5 nm s^{-1}, respectively, and a pressure of 1.0 × 10^{-6} Torr.

Preparation of SAMs: The gold-coated coverslips were immersed in 1 mM of BAT:HO-PEG-alkyl-SH (1:9) or **1**: HO-PEG-alkyl-SH (1:9) in EtOH for 16 h at room temperature. The substrates were washed with deionified ultrafiltered water and ethanol and then dried under N$_2$.

The incubations with neutravidin, biotin peptide derivatives, and the antibodies were carried out under the same conditions as above. After all incubations, a drop of the matrix 2′,4′,6′-trihydroxyacetophenone monohydrate (THAP) diluted in acetone (30 mg mL^{-1}) was deposited on the gold spot. After evaporation of the drop, all the peptides on the spots were characterized by SAMDI using a 4800 MALDI-TOF/TOF (Applied Biosystems, Framingham, MA).

Adhesion Pull-off Experiments: Force spectroscopy studies were performed using a Molecular Force Probe 3D microscope (Asylum Research, Santa Barbara, CA, USA). Silicon nitride tips on triangular cantilevers were obtained from Olympus. The tips were functionalized with (3-mercaptopropyl)triethoxysilane, during 1 h under vacuum. Then the tip was incubated with a 1 mM aqueous solution of maleimidopropionyl-PEG-*N*-hydroxysuccinimyl (MIP-PEG-NHS) ester overnight at room temperature. The maleimide was attached to the free thiol of the silane on the tip, and the NHS was attached to a free amine of the antibody.[47] The last incubation was performed with the anti-p53 or anti-HSA in a 0.5 mg mL^{-1} concentration in PBS during 1 h at room temperature. The gold surfaces were directly deposited overnight onto gold-coated glass surfaces prepared by the template-stripped gold method.[48] The gold surfaces were then stamped by microcontact printing for BAT and **1**

and then immersed in a HS-PEG-OH in EtOH solution as described above. An image of the pattern by contact AFM in liquid was obtained, with the tip functionalized. Then, on the same area, we performed an adhesion pull-off force assay. For each image, 4096 force plots were recorded and compiled in a 4096-pixel image of the pattern in terms of force (so-called force map). Data analysis and statistical treatments were carried out using the software provided by the AFM manufacturer (IgorPro 6.20; WaveMetrics Inc., Lake Oswego, OR, USA). To restrict the analysis to single-molecule interactions, the peak selection was carried out manually, setting a maximum length threshold of 100 nm (which corresponds to the maximum length of the PEG linker), considering only the last adhesion event of the force extension curves. The curves that did not attain this length were considered as non-specific adhesion.

Impedance Measurements: (The microelectrode fabrication for the impedance measurements is elaborated in the Supporting Information (S10).) The electrochemical measurements were carried out at room temperature in a conventional voltammetric cell with a three-electrode configuration. A Solartron 1260 and an impedance analyzer with Solartron 1287 potentiostat were used. The chips used consisted of five gold electrodes, four with a round shape of 100 μm, 50 μm, 20 μm, and 10 μm, and one with a T-shape (Supporting Information, S6). For all quantitative experiments, we used the 100 μm-electrode as a working electrode, and two external electrodes, namely, platinum foil (Ecochemie, Utrecht, The Netherlands) as a counter electrode and Ag/AgCl as the reference electrode (Metrohm, Herisau Switzerland). Previous to SAM formation, the electrodes were activated by performing ten cycles of chronoamperometry from −2V to 0V in a PBS solution. Then, cyclic voltammetry in 20 mM $K_4Fe(CN)_6$ solution in PBS buffer was carried out in order to check the gold surfaces and obtain the DC point (the constant potential point at which further impedance experiments would be carried out). The chips were rinsed with acetone, isopropanol, and ethanol, and then dried under nitrogen. The impedance spectra were obtained in a frequency range from 0.1 Hz to 100 KHz, using a DC voltage of −0.5 V and an AC voltage of 10 mV. As a test fluid for impedance measurements, we used 20 mM $K_4Fe(CN)_6$ solution in PBS buffer.

The incubations with **1** and BAT were performed as previously described for the preparation of SAMs.

Subsequent incubations of anti-p53 in PBS at concentrations of 10^{-17}, 10^{-14}, 10^{-10}, and 10^{-8} M were performed for 2 h. Also, we incubated the anti-p53 in undiluted serum at 10^{-12} M for 2 h in another chip. Other incubations with anti-HSA at 10^{-8} M during 2 h were also carried out.

The R_{ct} (charge-transfer resistance) of all the concentrations was analyzed and fitted with the corresponding circuit using Zview software (Supporting Information, S11). The R_{ct} of the concentrations used in each experiment was normalized versus the R_{ct} of the SAM reference to obtain an indicator that could be compared between the different experiments (Supporting Information, S9).

Supporting Information

Supporting Information is available from the Wiley Online Library or from the author.

[1] B. Morón, M. T. Bethune, I. Comino, H. Manyani, M. Ferragud, M. C. López, Á. Cebolla, C. Khosla, C. Sousa, *PLoS ONE* **2008**, *3*, e2294.

[2] H. T. Tan, J. Low, S. G. Lim, M. C. M. Chung, *FEBS J.* **2009**, *276*, 6880.

[3] W. Boukouaci, M. Busson, R. Peffault de Latour, V. Rocha, C. Suberbielle, D. Bengoufa, N. Dulphy, P. Haas, C. Scieux, H. Amroun, E. Gluckman, R. Krishnamoorthy, A. Toubert, D. Charron, G. Socie, R. Tamouza, *Blood* **2009**, *114*, 5216.

[4] N. Rifai, M. A. Gillette, S. A. Carr, *Nat. Biotechnol.* **2006**, *24*, 971.

[5] V. V. Levenson, *BBA-Gen. Subjects* **2007**, *1770*, 847.

[6] L. Feng, L. Wu, J. Wang, J. Ren, D. Miyoshi, N. Sugimoto, X. Qu, *Adv. Mater.* **2012**, *24*, 125.

[7] T. Soussi, *Cancer Res.* **2000**, *60*, 1777.

[8] S. Hanash, *Nature* **2003**, *422*, 226.

[9] J.-M. Portefaix, C. Fanutti, C. Granier, E. Crapez, R. Perham, J. Grenier, B. Pau, M. Del Rio, *J. Immunol. Methods* **2002**, *259*, 65.

[10] C.-P. Jia, X.-Q. Zhong, B. Hua, M.-Y. Liu, F.-X. Jing, X.-H. Lou, S.-H. Yao, J.-Q. Xiang, Q.-H. Jin, J.-L. Zhao, *Biosens. Bioelectron.* **2009**, *24*, 2836.

[11] G. Yan, D. Xing, S. Tan, Q. Chen, *J. Immunol. Methods* **2004**, *288*, 47.

[12] M. Askari, J. P. Alarie, M. Moreno-Bondi, T. Vo-Dinh, *Biotechnol. Progr.* **2001**, *17*, 543.

[13] L. Feng, Y. Chen, J. Ren, X. Qu, *Biomaterials* **2011**, *32*, 2930.

[14] J. S. Daniels, N. Pourmand, *Electroanalysis* **2007**, *19*, 1239.

[15] H. Huang, Z. Liu, X. Yang, *Anal. Biochem.* **2006**, *356*, 208.

[16] D. P. Lane, *Nature* **1992**, *358*, 15.

[17] V. Goodell, l. G. Salazar, N. Urban, C. W. Drescher, H. Gray, R. E. Swensen, M. W. McIntosh, M. L. Disis, *J. Clin. Oncol.* **2006**, *24*, 762.

[18] A. Gadducci, M. Ferdeghini, F. Buttitta, S. Cosio, A. Fanucchi, C. Annicchiarico, O. Gagetti, G. Bevilacqua, A. R. Genazzani, *Gyneacol. Oncol.* **1999**, *72*, 76.

[19] R. Broll, M. Duchrow, E. Oevermann, C. Wellm, O. Schwandner, H. Schimmelpenning, U. J. Roblick, H. P. Bruch, U. Windhövel, *Int. J. Colorectal Dis.* **2001**, *16*, 22.

[20] M. Lechpammer, J. Lukač, S. Lechpammer, D. Kovačević, M. Loda, Z. Kusić, *Int. J. Colorectal Dis.* **2004**, *19*, 114.

[21] S. Metcalfe, T. K. Wheeler, S. Picken, S. Negus, A. J. Milner, *Breast Cancer Res.* **2000**, *2*, 438

[22] L. Harris, H. Fritsche, R. Mennel, L. Norton, P. Ravdin, S. Taube, M. R. Somerfield, D. F. Hayes, R. C. Bast, Jr, *J. Clin. Oncol.* **2007**, *25*, 5287.

[23] C. Chapman, A. Murray, J. Chakrabarti, A. Thorpe, C. Woolston, U. Sahin, A. Barnes, J. Robertson, *Ann. Oncol.* **2007**.

[24] K. S. Anderson, N. Ramachandran, J. Wong, J. V. Raphael, E. Hainsworth, G. Demirkan, D. Cramer, D. Aronzon, F. S. Hodi, L. Harris, T. Logvinenko, J. LaBaer, *J. Proteome Res.* **2008**, *7*, 1490.

[25] L. Zhong, K. Ge, J.-c. Zu, L.-h. Zhao, W.-k. Shen, J.-f. Wang, X.-g. Zhang, X. Gao, X. Hu, Y. Yen, K. Kernstine, *Breast Cancer Res.* **2008**, *10*, R40.

[26] M. Müller, M. Meyer, T. Schilling, E. Ulsperger, T. Lehnert, H. Zentgraf, W. Stremmel, M. Volkmann, P. Galle, *Int. J. Oncol.* **2006**, *29*, 973.

[27] C. W. Stephen, P. Helminen, D. P. Lane, *J. Mol. Biol.* **1995**, *248*, 58.

[28] P. Lloyd-Williams, F. Albericio, E. Giralt, *Chemical Approaches to the Synthesis of Peptides and Proteins*, CRC, Boca Raton, FL **1997**.

[29] A. Kumar, H. A. Biebuyck, G. M. Whitesides, *Langmuir* **1994**, *10*, 1498.

[30] J. L. Wilbur, A. Kumar, E. Kim, G. M. Whitesides, *Adv. Mater.* **1994**, *6*, 600.

[31] A. Kumar, G. M. Whitesides, *Appl. Phys. Lett.* **1993**, *63*, 2002.

[32] E. Prats-Alfonso, F. García-Martín, N. Bayo, L. J. Cruz, M. Pla-Roca, J. Samitier, A. Errachid, F. Albericio, *Tetrahedron* **2006**, *62*, 6876.

[33] A. Ulman, M. Ioffe, F. Patolsky, E. Haas, D. Reuvenov, *J. Nanobiotechnol.* **2011**, *9*, 26.

[34] M. Mrksich, *ACS Nano* **2008**, *2*, 7.

[35] M. Hassan, E. Azzazy, R. H. Christenson, *All About Albumin: Biochemistry, Genetics, and Medical Applications*, Academic Press, San Diego, CA **1997**.

[36] X. Sisquella, K. de Pourcq, J. Alguacil, J. Robles, F. Sanz, D. Anselmetti, S. Imperial, X. Fernàndez-Busquets, *FASEB J.* **2010**, *24*, 4203.

[37] J. Farrera-Sinfreu, E. Giralt, S. Castel, F. Albericio, M. Royo, *J. Am. Chem. Soc.* **2005**, *127*, 9459.

[38] A. Bogomolova, E. Komarova, K. Reber, T. Gerasivov, O. Yavuz, S. Bhatt, M. Aldisi, *Anal. Chem.* **2009**, *81*, 3944.

[39] B.-Y. Chang, S.-M. Park, *Annu. Rev. Anal. Chem.* **2010**, *3*, 207.

[40] J. C. Pyun, S. D. Kim, J. W. Chung, *Anal. Biochem.* **2005**, *347*, 227.

[41] R. Y. Lai, D. S. Seferos, A. J. Heeger, G. C. Bazan, K. W. Plaxco, *Langmuir* **2006**, *22*, 10 796.

[42] R. Dolling, M. Beyermann, J. Haenel, F. Kernchen, E. Krause, P. Franke, M. Brudel, M. Bienert, *Chem. Commun.* **1994**, 853.

[43] J. Fernández-Carneado, E. Giralt, *Tetrahedron Lett.* **2004**, *45*, 6079.

[44] R. Fischer, O. Mader, G. N. Jung, R. Brock, *Bioconjugate Chem.* **2003**, *14*, 653.

[45] B. T. Houseman, E. S. Gawalt, M. Mrksich, *Langmuir* **2002**, *19*, 1522.

[46] Z. A. Gurard-Levin, M. Mrksich, *Biochemistry* **2008**, *47*, 6242.

[47] M. C. Garnett, *Adv. Drug Delivery Rev.* **2001**, *53*, 171.

[48] M. Hegner, P. Wagner, G. Semenza, *Surf. Sci.* **1993**, *291*, 39.